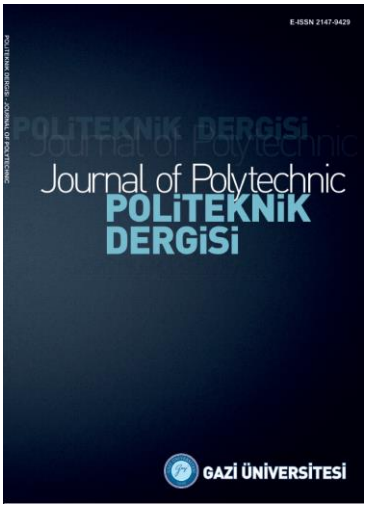

POLİTEKNİK DERGİSİ

JOURNAL of POLYTECHNIC

ISSN: 1302-0900 (PRINT), ISSN: 2147-9429 (ONLINE)
URL: http://dergipark.org.tr/politeknik

Investigation of the abrasive wear behavior of GFRC and CFRC with different parameters using taguchi and artificial neural networks method

GFRC ve CFRC'nin abrasiv aşınma davranışının taguchi ve yapay sinir ağları yöntemi kullanılarak farklı parametrelerde incelenmesi

Yazar(lar) (Author(s)): *Mehmet Emin DEMİR[1]*

ORCID[1]: 0000-0001-9630-6378

To cite to this article:."Investigation Of The Abrasive Wear Behavior Of GFRC And CFRC with Different Parameters Using Taguchi And Artificial Neural Networks Method", ***Journal of Polytechnic***, *(*): *, (*).

Bu makaleye şu şekilde atıfta bulunabilirsiniz:. "Investigation Of The Abrasive Wear Behavior Of GFRC And CFRC with Different Parameters Using Taguchi And Artificial Neural Networks Method", ***Politeknik Dergisi***, *(*): *, (*).

Erişim linki (To link to this article): http://dergipark.org.tr/politeknik/archive

DOI: 10.2339/politeknik.1444907

Investigation of The Abrasive Wear Behavior of GFRC and CFRC with Different Parameters Using Taguchi and Artificial Neural Networks Method

Highlights

- *In abrasive wear tests conducted on composite materials, the friction coefficients of GFRC were found to be lower than those of CFRC at different loads, sliding distances, and sliding speeds.*
- *The conducted Taguchi analysis revealed that the lowest coefficient of friction was achieved with glass fiber type under a load of 10 N, a sliding distance of 500 m, and a sliding speed of 0.4 m/s. The increase in applied load beyond a certain level has resulted in an increase in the coefficient of friction.*
- *The Taguchi analyses and ANN modeling have demonstrated the consistency of the experimental results. The ANN model has exhibited a more successful performance than the Taguchi method in predicting mass loss and Coefficient of Friction values.*

Graphical Abstract

Abrasive wear tests were conducted using two different fiber-reinforced composites. The results obtained from experiments conducted at different wear parameters were analyzed using the Artificial Neural Network and Taguchi methods. Experimental stage is given in figure 1.

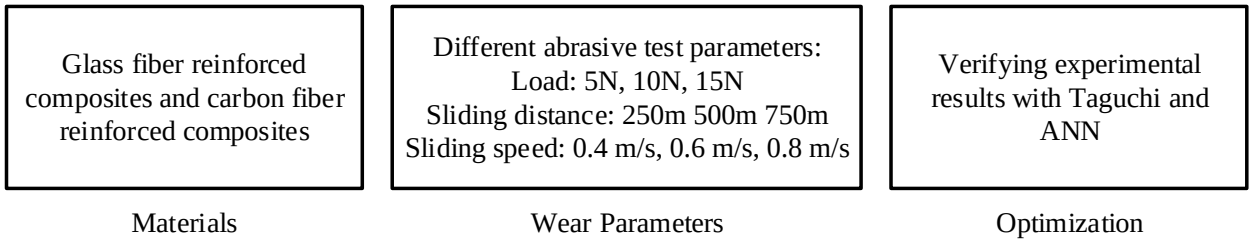

Figure. Experimental process

Aim

This study aims to experimentally determine the effect of different wear parameters and levels applied to two different fiber types on tribological behavior and validate them with numerical analysis.

Design & Methodology

Different fiber types were subjected to abrasive wear tests using sandpaper in a pin-on-disk wear testing machine.

Originality

Experimental wear tests were conducted on different fiber types with varying parameters, and the obtained results were analyzed using both Taguchi experimental design and artificial neural networks (ANNs) to investigate the consistency of the results.

Findings

It was observed that increasing the applied load, sliding distance, and sliding speed had a detrimental effect on both the coefficient of friction (COF) and mass loss for both types of fibers subjected to abrasion.

Conclusion

Low applied load, sliding distance, and speed result in lower mass loss and lower coefficient of friction (COF) for the abraded fibers. The experimental results obtained from both Taguchi and ANN (Artificial Neural Network) analyses reveal consistency.

Declaration of Ethical Standards

The author(s) of this article declare that the materials and methods used in this study do not require ethical committee permission and/or legal-special permission.

Investigation of The Abrasive Wear Behavior of GFRC and CFRC with Different Parameters Using Taguchi and Artificial Neural Networks Method

Araştırma Makalesi / Research Article

Mehmet Emin Demir[1*]

Batman University, Beşiri Organized Industrial Zone Vocational School, Batman, Turkey,

(Geliş/Received:29.02.2024 ; Kabul/Accepted :18.04.2024 ; Erken Görünüm/Early View :02.07.2024)

ABSTRACT

Fiber-reinforced composites are increasingly being utilized in various sectors, including aerospace, maritime, electronic components, and in elements exposed to wear such as bolts, nuts, cams, and gaskets. This study aims to determine the optimal processing parameters in abrasive wear tests conducted under varying wear conditions on glass and carbon fiber-reinforced composites. Employing a mixed-level L36 Taguchi orthogonal experimental design, tests were conducted on a pin on disk apparatus under different loads, sliding distances, and speeds. In the experiments, four different parameters were utilized: fiber type, applied load, sliding distance, and sliding velocity. Three different levels were applied for load (5N, 10N, 15N), sliding distance (250m, 500m, 750m), and sliding velocity (0.4m/s, 0.6m/s, 0.8m/s). The results indicated that the most significant parameters affecting the coefficient of friction (COF) and mass loss were the type of fiber and the load. It was observed that an increase in load, sliding distance, and speed augmented the COF and mass loss. Predictions of the coefficient of friction and mass loss were made using a model developed in Artificial Neural Networks (ANN), and these predictions were compared with experimental results. The R^2 overall regression values for COF and mass loss in ANN were calculated as 0.98939 and 0.98349, respectively. ANN was found to provide more consistent results in predicting COF and mass loss compared to the Taguchi method.

Keywords: GFRC, CFRC, Abrasive wear, Taguchi, ANN

GFRC ve CFRC'nin abrasiv aşınma davranışının taguchi ve yapay sinir ağları yöntemi kullanılarak farklı parametrelerde incelenmesi

ÖZ

Fiber takviyeli kompozitler, havacılık, denizcilik, elektronik bileşenler ve cıvata, somun, kam ve conta gibi aşınmaya maruz kalan elemanlar gibi çeşitli sektörlerde giderek daha fazla kullanılmaktadır. Bu çalışma, cam ve karbon fiber takviyeli kompozitler üzerinde farklı aşınma koşullarında yapılan aşındırıcı aşınma testlerinde optimal işleme parametrelerini belirlemeyi amaçlamaktadır. Karışık düzeyli L36 Taguchi ortogonal deneysel bir tasarım kullanılarak, farklı yükler, kayma mesafeleri ve hızlar altında bir pim üzerinde disk cihazında testler gerçekleştirilmiştir. Deneylerde elyaf tipi, uygulanan yük, kayma mesafesi, kayma hızı olmak üzere 4 farklı parametre kullanılmıştır. Yük (5N,10N, 15N), kayma mesafesi (250m, 500m, 750m) ve kayma hızında (0.4m/s, 0.6m/s, 0.8m/s) ise 3 farklı seviye uygulanmıştır. Sonuçlar, sürtünme katsayısı (COF) ve kütle kaybını etkileyen en önemli parametrelerin fiber tipi ve yük olduğunu göstermiştir. Yükün, kayma mesafesinin ve hızın artmasıyla COF ve kütle kaybının arttığı gözlemlenmiştir. Sürtünme katsayısı ve kütle kaybı için yapay sinir ağları (ANN) ile geliştirilen bir model kullanılarak tahminlerde bulunulmuş ve bu tahminler deneysel sonuçlarla karşılaştırılmıştır. ANN'deki COF ve kütle kaybı için R2 genel regresyon değerleri sırasıyla 0.98939 ve 0.98349 olarak hesaplanmıştır. ANN'nin COF ve kütle kaybını tahmin etmede Taguchi yöntemine göre daha tutarlı sonuçlar sağladığı bulunmuştur.

Anahtar kelimeler: GFRC, CFRC, Abrasive aşınma, Taguchi, ANN

1. INTRODUCTION

Polymer matrix composite materials are extensively used for their attributes such as high strength, low density, ease of production, cost-effectiveness, chemical stability, and superior corrosion resistance. Correct design and manufacturing of the reinforcing element and matrix in composites can lead to the matrix materials like epoxy, polyester, phenolic, and vinyl ester are commonly employed in these composites. [1-4] However, in many structural applications, the tribological and mechanical properties of polymer materials are inadequate. Compared to metals and ceramics, polymers exhibit considerably lower hardness. Reinforcement of these polymers with fibers in various

*Sorumlu Yazar (Corresponding Author)

e-posta : memin.demir@batman.edu.tr

fabric or particulate forms has been highly successful in addressing these shortcomings. While the polymer matrix ensures the cohesion of fibers and protection against external influences, the fibers contribute to load transfer and enhance hardness of the material [5]. High shear strength and hardness of reinforcing fibers enhance strength and wear resistance of the composites [6]. Furthermore, the type, orientation, and quantity of fibers used alter the properties of fiber-reinforced composites. Presently, various synthetic fiber types such as glass, carbon, and aramid are widely utilized in polymer materials [7]. These composite materials are increasingly favored in wear-prone areas due to their excellent lubrication properties, superior wear resistance, and low coefficient of friction [8,9]. Fiber-reinforced composites have found widespread application in diverse sectors including automotive manufacturing, wind turbines, roller bearings, and ship components [10,11].

Tribology defines the relationships of wear and friction between relatively moving objects according to parameters like load, material type, temperature, friction surface, and density [12-14]. In wear-related studies, the Taguchi method is frequently utilized to identify optimal parameters for reducing number of experiments and minimizing the COF and wear loss [15]. Alongside Taguchi experimental design, other models such as regression analysis and ANN are also utilized. [16,17]. The utilization of ANN's in engineering extends beyond tribology, encompassing the analysis and resolution of various issues in different fields such as determining optimal parameters in machining processes, calculating stress concentration factors, or enhancing efficiency in the energy sector [54-57]. Scientific studies have proven that ANNs provide higher accuracy than other analytical methods and exhibit a stronger correlation between predicted and experimental values [18,19]. Due to the extensive use of glass and carbon fibers in tribological applications, researchers have conducted numerous studies using Taguchi experimental design and ANN to determine the wear behavior of these composites under various parameters [20-23].

Sharma and colleagues experimentally investigated the wear behavior of graphene-filled glass fiber-reinforced composites (GFRC) under various loads and filler ratios. They observed that the wear rate and COF in 1% graphene-filled composites significantly decreased compared to unfilled composites. The ANOVA results indicated that the amount of graphene filler had a greater impact on COF and wear rate than the load. Their analysis using ANN showed a congruence between predicted and experimental values [10]. Yadav and team studied the erosion wear behavior of Al_2O_3 filled GFRC at three different filler ratios. Using the Taguchi experimental design to identify the most influential parameter on wear, they found from ANOVA results that the impact velocity was the most significant factor. They determined that the lowest and highest erosion wear occurred in composites with 10% filler and without filler, respectively [24]. Kumar et al. [25] evaluated the effect of filler content, sliding speed, load, and sliding distance on the wear behavior of nano-clay filled E-glass reinforced composite materials using Taguchi analysis. ANOVA results showed that the addition of fibers to the layers had a significant impact on the coefficient of friction. They identified the filler ratio as the most crucial parameter affecting the wear resistance of fiber-reinforced composites. Paturkar and colleagues analyzed the effects of different loads, sliding distances, and speeds on jute reinforced epoxy and jute/glass reinforced epoxy composites using the Taguchi method. They applied variance analysis to determine the relationship between applied parameters and wear rates, finding that the combined use of jute and glass fibers increased the composite's wear resistance. Variance analysis revealed that the most significant parameters in wear experiments were load, sliding speed, and sliding distance, respectively. Karthik and others investigated the impact of varying carbon fiber ratios on wear behavior of glass and kevlar reinforced composites. They observed that the wear rate decreased as the sliding speed increased, suggesting that at higher speeds, the composite's transfer layer acted as a protective coating, thereby reducing wear rate. Taguchi analysis identified sliding speed as the most effective parameter and load as the weakest [26]. Ravichandran et al. used Taguchi experimental design to examine the impact of filler ratio, load, wear duration on Halloysite nanotube (HNT) filled GFRC. They concluded that the filler ratio was the most effective parameter in reducing wear rate, with the load being the least effective. SEM images of worn surfaces were consistent with the test results [27]. Bagci and team analyzed the effect of different fiber orientation angles and SiO_2 filler ratios on the erosion wear behavior of GFRC using the Taguchi method. They identified the effectiveness levels of parameters on erosion wear amount as impact angle, impact velocity, fiber direction, and filler amount, respectively [28]. Thimmaiah and colleagues used Taguchi and ANN models to analyze the wear behavior of kenaf and Kevlar reinforced composites with different stacking sequences. They discovered that composites with kenaf in the outer layers exhibited an increase in wear rate as the load increased. ANN analysis showed that the predicted values were close to the experimental results [29].

When studies related to CFRC and GFRC are examined, it is noted that there is a limited number of researches that experimentally investigate both glass and carbon fiber-reinforced composites and subsequently analyze the results obtained from these experiments using various optimization tools. In this context, it would be beneficial to obtain optimal parameters in the experimental study, which utilizes four different factors and three different levels, through widely used techniques such as Taguchi and ANN, and to compare and validate the experimental results with the analysis results. In this study, the impact of load, sliding distance, and sliding speed on the wear behavior of GFRC and CFRC materials was examined

utilizing both Taguchi experimental design and ANN method.

2. MATERIAL AND METHOD

GFRC and CFRC, commercially available, were utilized in experimental investigations. The obtained GFRC and CFRC samples have a fiber content of 75% by weight and a resin content of 25% by weight. Vinyl ester resin was employed as the matrix material. The densities of GFRC and CFRC are 1.85 g/cm³ and 1.53 g/cm³, respectively. The samples commercially procured have lengths of 100 mm and diameters of 10 mm. To facilitate attachment to the testing apparatus, rods of 30 mm length were cut from 1 m long bars. The fibers employed in GFRC and CFRC are continuous fibers and should be oriented longitudinally. The composite samples, attached to the pin of the wear device, were abraded under specified loads, sliding distances, and speeds on sandpaper adhered to a rotating table. Abrasive wear tests on GFRC and CFRC composite materials were conducted using 400 grit silicon carbide sandpaper as the abrasive material. The tests were conducted using a pin on disk wear apparatus under dry situations according to ASTM G99 standards. After each test, the sandpaper was replaced for a new test. The rotational speed of the device was adjusted with a tachometer. Data related to the COF were transferred to a computer connected to the device and converted into graphs. The test samples used in the experiments and the experimental setup are shown in Figure 1. Some mechanical and physical properties of the test samples are illustrated in Table 1.

Table 1. Mechanical and pysical properties of GFRC and CFRC composites

Composite Type	GFRC	CFRC
Tensile Strength (MPa)	1000	2080
Compressive Strength (MPa)	550	1450
Tensile Module (GPa)	38	145
Density (g/cm^3)	1.8	1.5

Mass loss, wear volume, wear rate, and specific wear rate are critical parameters used to determine the extent of wear. Parameters such as sliding distance, load, lubrication, and sliding speed are significant influencers on these parameters [30]. For GFRC and CFRC, the determination of wear amount primarily relies on mass loss. The samples were weighed on a precision scale before and after the experiments to ascertain the difference in their weights. To reduce the number of repetitive experiments, thereby saving time, and to determine the optimum experimental parameters, both the Taguchi orthogonal experimental design and the ANN method have been employed. The effectiveness of different parameters on wear behavior has been presented utilizing Signal to Noise (S/N) ratio and ANOVA method. Table 2 illustrates the application of a four-factor mixed-level L36 (2^1-3^3) Taguchi design in the experimental studies.

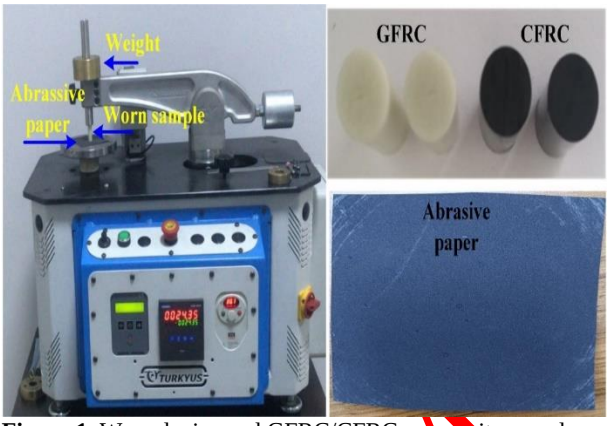

Figure 1. Wear device and GFRC/CFRC composite samples

Taguchi and variance analyses were conducted using the Minitab software. In the Taguchi analyses, S/N ratio was selected as "the smaller the better." This ratio was calculated using Equation 1 provided below [45].

$$\frac{S}{N} = -10log\left(\frac{\sum y^2}{n}\right) \quad (1)$$

Where, $\frac{S}{N}$: Signal to noise ratio, y: observed value, n: Observation number

Table 2. Control factors and levels used in wear test

Factor	Level-1	Level-2	Level-3
Fiber Type	Glass	Carbon	
Applied Load	5N	10N	15N
Sliding Distance	250m	500m	750m
Sliding Speed	0.4m/s	0.6m/s	0.8m/s

3. WEAR TEST RESULTS

In both GFRC and CFRC, the load applied, sliding distance, and sliding speed are significant parameters that affect the COF and mass loss. Figure 2 presents the graph of the COF obtained at different loads for GFRC and CFRC, as measured by the device.

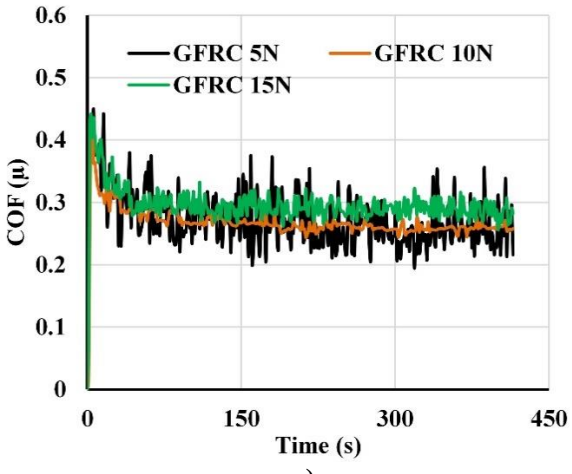

a)

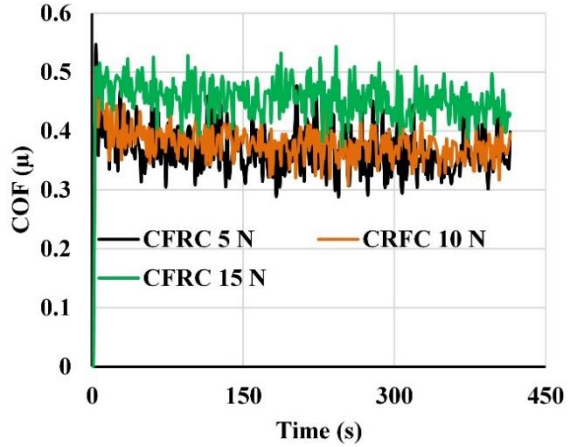

b)

Figure 2. Load-dependent friction coefficient graph at 0.6 m/s and 250 m; a) GFRC, b) CFRC

Upon examining the graph, it is apparent that the COF for GFRC are lower than those for CFRC. In Figure 2a, it is observed that at a load of 5N, the wavelengths in GFRC are higher compared to other loads. When the load is increased to 10N, there is a significant drop in the wavelengths, and at 15N, they begin to increase slightly. In Figure 2b, it is noted that COF increases with the load, with the highest fluctuation and the highest COF for CFRC occurring at a load of 15N. At a speed of 0.6 m/s, a load of 5N, and a sliding distance of 250 meters, the COF for GFRC is recorded at 0.27 μ, while for CFRC, it is 0.36 μ. It can be said that initially, at low loads, there is more fluctuation and an increase in the friction coefficient due to the temperature-dependent plasticization in the matrix. It can also be said that particles detached from the material adhere to the abrasive surface, disrupting the surface integrity of the counterface, thus leading to an increase in the friction coefficient [52,53].

Some studies have found that the COF decreases with increasing load. This phenomenon is explained by a thin film layer formation of on composite surface caused by plastic deformation of the matrix, which acts as a lubricant [30-32]. However, beyond a critical value of the load, the material experiences an increase in temperature due to the increased frictional force. This rise in temperature can weaken the epoxy polymer molecular chains, resulting in an increase in the COF. [33,34]. Figure 3 displays the changes in the COF and mass loss for GFRC and CFRC in relation to the applied load. It has been determined that for both types of fibers, an increase in load leads to an increase in both COF and mass loss. For GFRC, increasing the load from 5N to 15N raised the COF from 0.27 μ to 0.29 μ. It was observed that at the same load, the COF value for CFRC was higher than that for GFRC. The higher hardness of CFRC, leading to particles breaking off during wear and getting trapped between the sandpaper and the sample, could be responsible for the higher COF and mass loss values in CFRC.

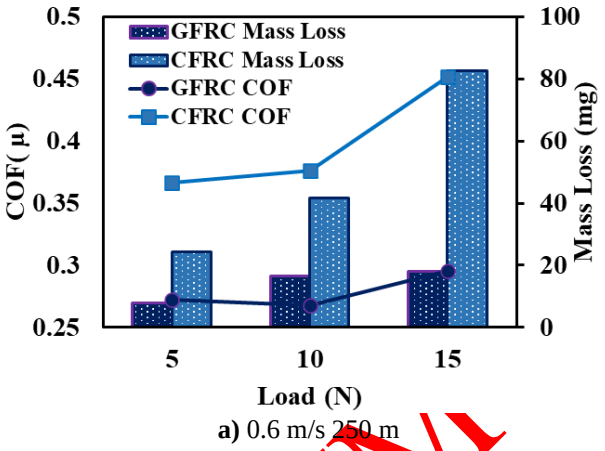

a) 0.6 m/s 250 m

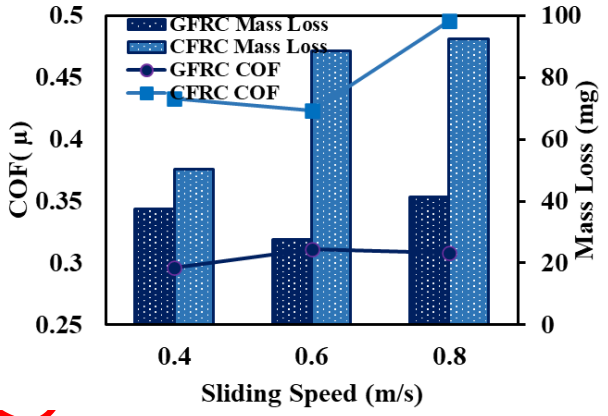

b) 15 N 500 m

Figure 3. Variation of COF and mass loss with load and sliding speed

This creates a third-body wear mechanism. In Figure 2, the lower fluctuation heights of GFRC's COF compared to CFRC and the stabilization of fluctuations after a certain wear duration support this explanation. Figure 3b shows that increasing the sliding speed negatively affects wear, increasing both the COF and mass loss. Raising the speed from 0.4 m/s to 0.6 m/s increased the COF values for GFRC and CFRC by 4% and 14%, respectively. In the study conducted by Sharma et al., it was noted that with increasing load in glass fiber reinforced composites, wear resistance decreases due to the increase in shear stresses [10]. Variance analysis (ANOVA) has been used to examine the effect of independent test variables on the composites COF. Table 3 presents the ANOVA results, showing the influence of different independent wear parameters on the dependent COF.

In Table 3, a P-value less than 0.05 point out that the independent variable is statistically considerable, meaning it substantially influences the optimal characteristic of the study. Accordingly, fiber type, load, and sliding speed are statistically significant, while sliding distance is not. An F-value greater than 4 for a factor suggests a significant effect of that variable on the studied characteristic.

Table 3. Analysis of Variance for SN ratios for COF

Source	DF	Seq SS	Adj SS	Adj MS	F	Cont.%	P
Fiber Type	1	52.75	52.75	52.77	228.4	79%	0.00
Load (N)	2	7.311	7.311	3.655	15.8	11%	0.00
Sliding Distance (m)	2	0.029	0.029	0.014	0.06	0.04%	0.93
Sliding Speed (m/s)	2	2.1275	2.1275	1.0637	4.61	3.36%	0.02
Residual Error	19	4.388	4.388	0.231		6.6%	
Total	26	66.61				100%	

Examining the F-value for the independent variables in relation to the dependent variable in the table, it is understood that the most influential parameters are, in order, fiber type, load, speed, and distance. According to Table 3, the fiber type provided the highest contribution at 79%.

Table 4 shows the levels and ranks of the independent variables for the dependent variable COF according to S/N ratio. This table helps in understanding the relative importance and impact of each variable on the COF, allowing for a more comprehensive analysis of the factors that contribute to wear in GFRC and CFRC materials.

Table 4. Response Table for S/N Ratios for COF

Level	Fiber Type	Load (N)	Sliding Distance (m)	Sliding Speed (m/s)
1	**10.811**	9.537	9.268	**9.496**
2	7.998	**9.690**	**9.275**	9.393
3		8.518	9.201	8.856
Delta	2.813	1.173	0.074	0.640
Rank	1	2	4	3

Upon reviewing Table 4, the optimum levels for achieving the best COF value are calculated as follows: fiber type at the first level (10.811), load at the second level (9.69), sliding distance at the second level (9.275), and sliding speed at the first level (9.496). The rank value in Table 4 indicates the order of importance of the independent variables on the COF. These are, in order, fiber type, load, sliding speed, and sliding distance.

Figure 4 presents S/N ratio graph, which illustrates the impact of fiber type and wear parameters on the COF during wear. Examining the Figure 4, the optimal COF values are achieved with glass fiber type, a load of 10 N, distance of 500 m, and speed of 0.4 m/s. When considering the effect of fiber type on COF, it is observed that GFRC has a lower COF compared to CFRC. The higher COF in CFRC, compared to GFRC, can be attributed to the abrasive particles detached from CFRC during wear tests, which act as abrasives between the contacting surfaces, thereby increasing the material's COF. In terms of the load's impact, the most suitable load for COF is found to be 10 N.

As the load increases, the COF initially decreases and then begins to rise again. This behavior can be attributed to the viscoelastic nature of polymers. Under applied load, the deformation in polymers is viscoelastic. The equation 2 representing the COF is $\mu = kN^{(n-1)}$ [35], where N represents load, k is a constant number, μ is COF, and n is a constant that ranges between 0.66 and 1. According to this equation, the COF decreases with an increase in load. However, beyond a certain threshold of load, an increase in the surface temperature at the contact area leads to an increase in the surface energy of the polymer and relaxation in the molecular chains, resulting in an increase in COF [31]. The impact of distance on the COF appears to be weaker compared to other parameters. Increasing the sliding distance from 250 m to 750 m does not cause a significant change in the COF. However, increasing sliding speed from 0.4 to 0.8 m/s has caused an increase in COF. This increase in COF due to higher sliding speeds can be explained by the reduction in contact stress [36].

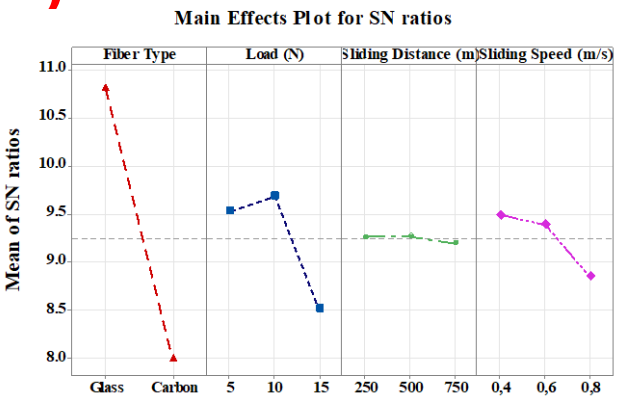

Figure 4. S/N ratio chart for COF

The most noticeable increase in COF is observed when speed changes from 0.6 to 0.8m/s. Consistent with the findings of this study, some research has indicated that the COF increases with higher speeds in abraded materials [32,37,38]. Contrarily, other studies have reported a decrease in COF with an increase in sliding speed, attributing it to the reduction in contact between the abraded material and the abrasive [39,40].

The normal probability graph showing the relationship of independent variables to dependent variables according to S/N ratios is provided in Figure 5. When examining the graph in Figure 5, it's observed that the residual values cluster around the linear line.

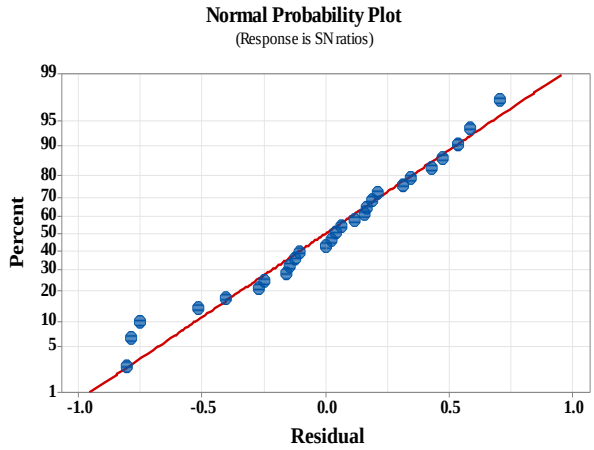

Figure 5. Regression plot for COF

This clustering suggests that the obtained R^2 results are consistent and reliable. Figure 5 includes a fitted line plot graphically comparing the experimental COF data with the estimated COF values.

Interpreting Figure 6, it is evident that the estimated values align well with the experimental results within a 95% confidence interval. The R^2 value is calculated as 90.3%, and the adjusted R^2 as 90%. These high R^2 values indicate a strong correlation and a good fit between the experimental data and the model predictions. The linear equation used to calculate the estimated COF values is provided below. This equation takes into account various parameters and their respective coefficients to predict the COF accurately.

$$COF\ (\mu) = 0.01053 + 0.9720 * Predicted \quad (2)$$

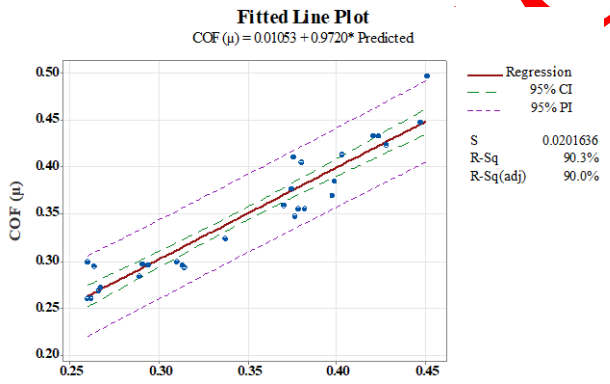

Figure 6. Fitted line plot of COF (μ)

To determine the order of importance and interactions of experimental parameters such as fiber type, load, sliding distance, and sliding speed on mass loss, a variance analysis (ANOVA) has been conducted on the experimental results. The ANOVA table for the S/N ratio of mass loss is presented in Table 5.

Upon examining the F-value in Table 5, it becomes clear that the most significant independent variables affecting mass loss are fiber type, load, sliding distance, and speed. The fact that the P-value for all independent variables is less than 0.05 at the end of the table indicates that all the main effects are statistically significant.

This analysis is crucial for understanding how different factors contribute to the wear behavior of materials, particularly in terms of mass loss. By identifying the most influential parameters, more efficient and effective improvements can be made to enhance the performance of composite materials under various conditions.

Table 5. ANOVA for S/N ratios for mass loss

Source	DF	Seq SS	Adj SS	Adj MS	F	P
Fiber Type	1	274.17	274.17	274.166	93.48	0.000
Load (N)	2	236.26	236.26	118.129	40.28	0.000
Sliding Distance (m)	2	152.18	152.18	76.091	25.95	0.000
Sliding Speed (m/s)	2	56.49	56.49	28.245	9.63	0.001
Residual Error	19	55.72	55.72	2.933		
Total	26	774.82				

In Table 6, the average S/N ratios for each level are provided. The 'Delta' value in the table represents the difference between the lowest and highest averages for each factor. Upon examining Table 6, the parameter combination that results in the lowest mass loss for the composite materials has been identified as glass fiber, a load of 5 N, a sliding distance of 250 m, and a sliding speed of 0.4 m/s. The rank value in Table 6 indicates the order of importance of the independent variables on mass loss. It is determined that load is the most influential parameter affecting mass loss, followed by fiber type, sliding distance, and sliding speed. This finding contrasts with Karthik's study on GFRC composites, where sliding distance was identified as the most influential parameter on wear rate, while load was considered the least effective parameter [24]. This discrepancy highlights how the impact of various parameters on wear behavior can vary depending on the specific material composition and testing conditions. It underscores the importance of conducting comprehensive analyses to tailor material properties and processing conditions to specific application requirements.

Table 6. Response Table for S/N ratios for mass loss

Level	Fiber Type	Load (N)	Sliding Distance (m)	Sliding Speed (m/s)
1	**-27.60**	**-27.08**	**-28.08**	**-29.61**
2	-34.01	-32.40	-31.55	-30.78
3		-34.01	-33.86	-33.09
Delta	6.41	6.92	5.78	3.48
Rank	2	1	3	4

Figure 7 illustrates the impact of four control parameters, each at 2 and 3 different levels, on mass loss. In the graph, the highest S/N ratio indicates the most ideal wear value. It is observed that the mass loss for glass fiber is less than that for carbon fiber.

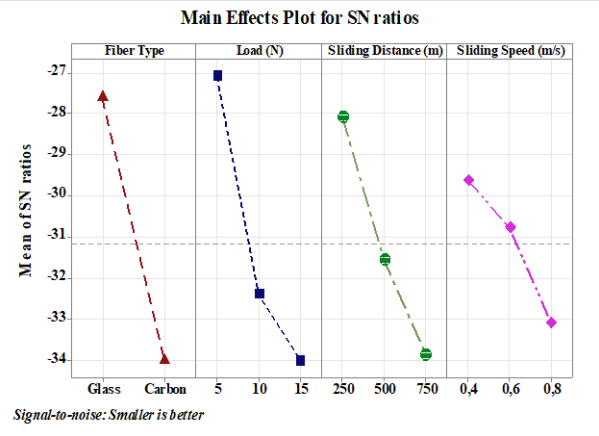

Figure 7. Effect of control parameters on mass loss

Additionally, an increase in load is correlated with an increase in mass loss, with the highest mass loss occurring at a load of 15 N. This increase in mass loss with higher loads can be attributed to the rise in temperature in the wear area, which causes the polymer surface to become plasticized, reducing the material's load-bearing capacity, accelerating part breakage, and consequently leading to increased mass loss. These findings are in line with results from other studies [12,41,42]. An increase in sliding speed also results in increased mass loss. The rise in temperature in the friction area due to increased sliding speed, along with increased shear and frictional thrust, are factors contributing to this increased mass loss. Results from similar studies support these findings [43,44]. According to the graph, the most ideal control parameters for minimizing mass loss are a fiber type of glass, a load of 5 N, a sliding distance of 250 m, and a sliding speed of 0.4 m/s. This combination of parameters seems to be most effective in reducing wear and tear, as indicated by the lower mass loss values.

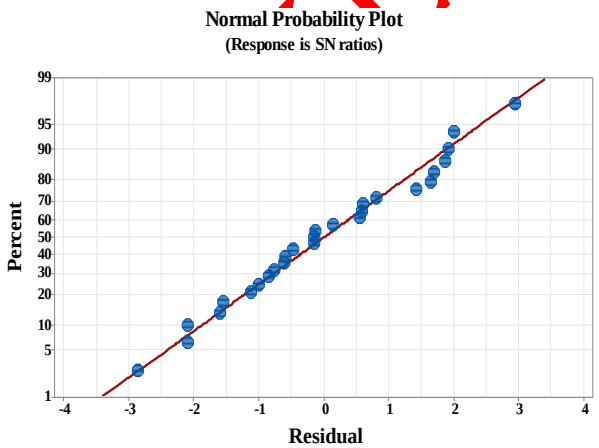

Figure 8. Regression graph of mass loss

In Figure 8, the residual plot for average mass loss is presented. In the normal probability graph, it is observed that the residual values are clustered close to the central value. This clustering of residuals, particularly at lower error magnitudes, suggests that the responses obtained from the data analysis are reliable and indicative of a good model fit. Figure 9 shows the fitted line plot for mass loss. It has been determined that the experimental results intersect with the predicted values at a 95% rate, demonstrating a strong correlation between observed and predicted mass loss. The R^2 value is calculated as 82.3%, and the adjusted R^2 as 81.7%. These high R^2 values indicate a substantial level of accuracy in the predictive model for mass loss. Equation 3 used to calculate the estimated mass loss values is provided below. This equation likely incorporates the different experimental parameters and their respective coefficients to accurately predict mass loss under various testing conditions.

$$\text{Mass loss (mg)} = 2.164+0.9341*\text{Predicted} \quad (3)$$

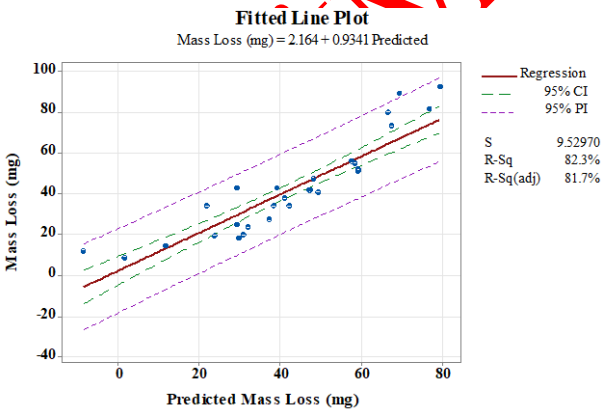

Figure 9. Fitted line plot of mass loss (mg)

Predictive models like ANN are among the most frequently used methods for saving time and cost. The flow chart of the feedforward ANN algorithm used for predicting mass loss and the COF is provided in Figure 10. This model comprises four inputs, ten hidden layers, and one output. The input consists of four neurons representing fiber type, load, sliding distance, and sliding speed. Output layer is refers to COF. In Figure 10, w and b refer LM backpropagation algorithm weights and bias respectively.

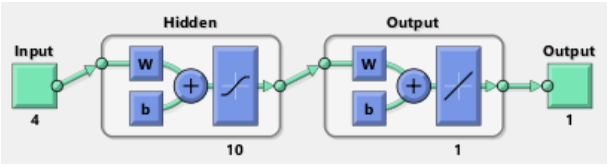

Figure 10. Flowchart of ANN

To achieve accurate outputs, the dataset needs to be trained, and the Mean Squared Error (MSE) must be calculated. The distribution of the dataset for training, validation, and testing is respectively 70%, 15%, and 15%. During the training of the ANN, the model attempts to decipher the relationship between the input and output parameters. For the prediction of COF and mass loss, the ANN model was developed using MATLAB R2016a software and the Levenberg-Marquardt algorithm. Levenberg-Marquardt algorithm method has been used due to its ability to provide faster analysis of engineering

problems compared to Bayesian Regularization algorithm, and Scaled Conjugate Gradient Descent[46]. This approach is effective in understanding and predicting the complex relationships between different variables in composite material wear, allowing for more precise and efficient design and testing of these materials.

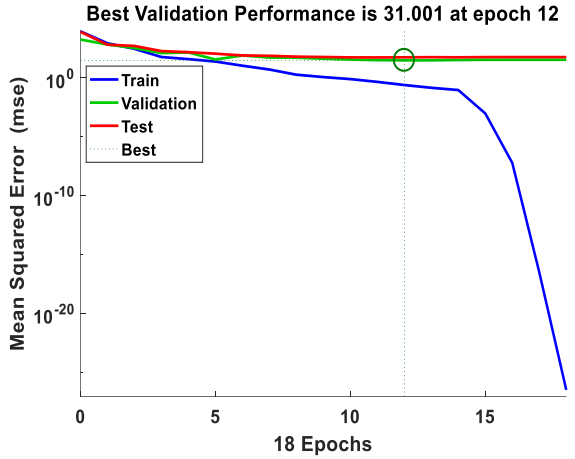

a) Mass Loss Performance

In Figure 11, MSE graph for the training, testing, and validation phases for mass loss and the COF is presented.

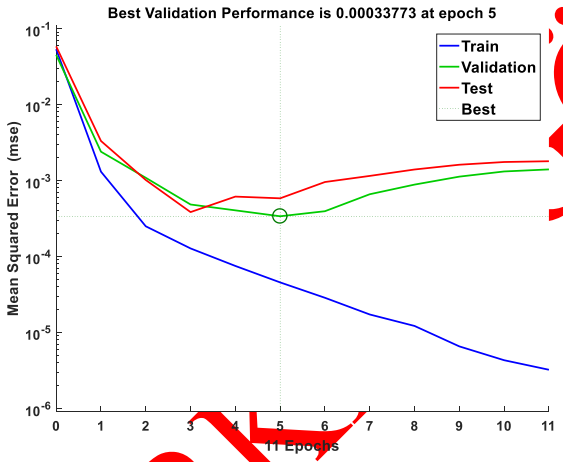

b) COF Performance

Figure 11. Performance graph for mass loss and COF

In Figure 11a, it can be seen that the training for mass loss concluded after 18 epochs. Additionally, the best MSE value was achieved at the 12th epoch, recorded as 31.001. This is the lowest MSE value obtained from five training trials for mass loss. In Figure 11b, for the regression analysis of COF, the data training ended after 11 epochs, and the best performance was observed at the 5th epoch with an MSE of 0.00033773 The close proximity of the MSE value for COF to zero indicates that the ANN model is well-trained and capable of producing predictions that are close to actual values. These results demonstrate the effectiveness of the ANN model in accurately predicting the wear behavior of composite materials under various conditions. The low MSE values signify a high level of precision in the model's predictions, making it a reliable tool for studying and understanding the wear characteristics of such materials. The error histogram graphs for mass loss and COF are shown in Figure 12 and Figure 13, respectively. Equation 4 has been used in the calculation of the error amount.

$$Error = Ti - Oi \quad (4)$$

Ti represents the predicted value, while Oi represents the actual value. Error histograms are obtained by subtracting the experimental values from the predicted values of the ANN under all conditions. In the mass loss error histogram in Figure 12, it can be observed that the error value is 0.00013. Many errors in the data set cluster around this value. It is understood that the largest error value does not exceed 0.51. The fact that the error value is very close to 0 also confirms the consistency of the network.

In the COF error histogram in Figure 13, it has been determined that the majority of the data set has an error value of 0.04856. The fact that this value is less than 1 indicates the accuracy of the ANN predictions.

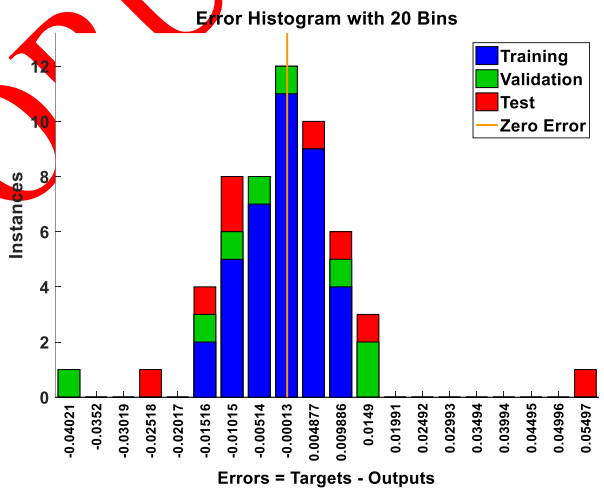

Figure 12. Error histogram of mass loss

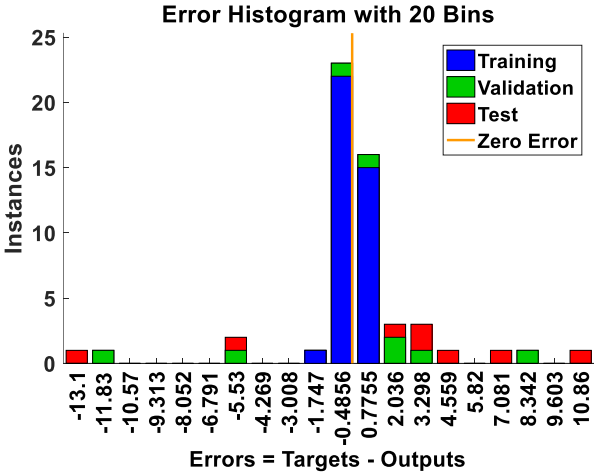

Figure 13. Error histogram of COF

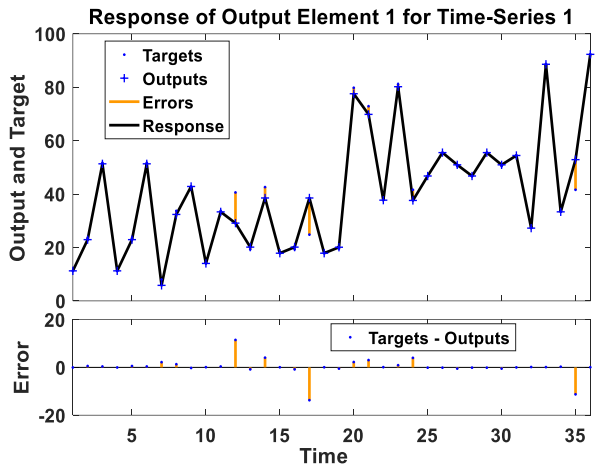

Figure 14. Residuals vs run of mass loss

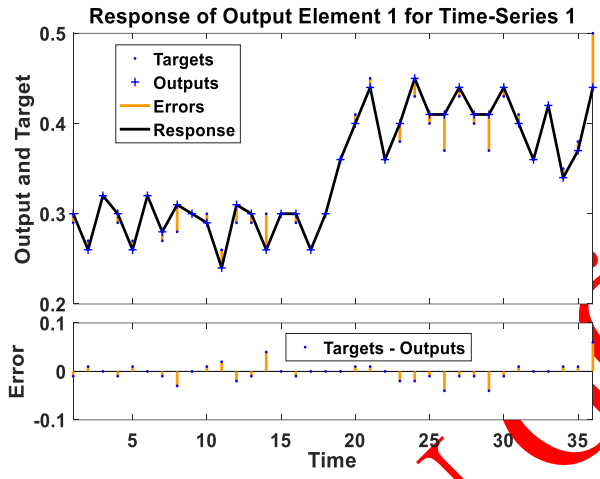

Figure 15. Residuals vs run of COF

Figure 14 and Figure 15 respectively show the target, output, and residue values for mass loss and COF in each run. When Figure 14, Figure 15 and Table 7 are evaluated together, it is observed that both mass loss and COF output values deviate by more than 5% from experimental results in 6 out of 36 runs. It is understood that remaining predicted values are obtained quite close to experimental values. Robust correlation is essential for validating the effectiveness of predictive models in simulating real-world scenarios. The ability of the ANN model to closely match the experimental data provides confidence in its use for future predictions and analyses in similar material testing and research scenarios. Figure 16 presents the mass loss regression graph of the ANN model for the training, validation, test, and all datasets combined. Upon examining the regression graph, it's observed that the coefficient of determination (R^2) for the training dataset is 0.9998, for validation is 0.9726, for testing is 0.968, and the overall model coefficient is 0.99036. The high coefficient of determination for the training dataset, being very close to 1, indicates a strong correlation and consistency between the experimental and predicted results.

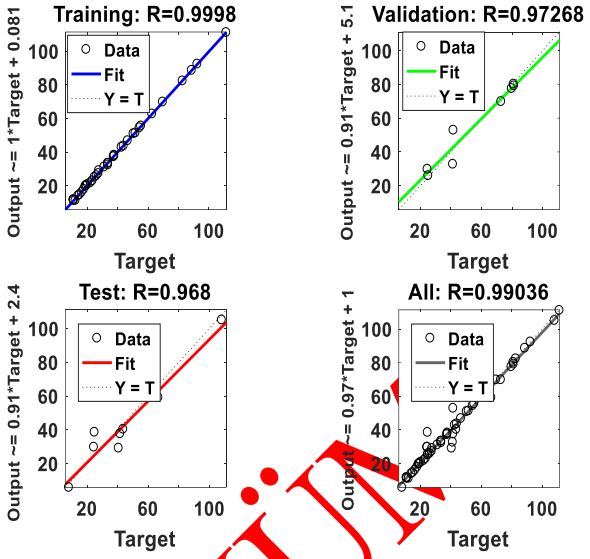

Figure 16. Regression Plot of Mass Loss

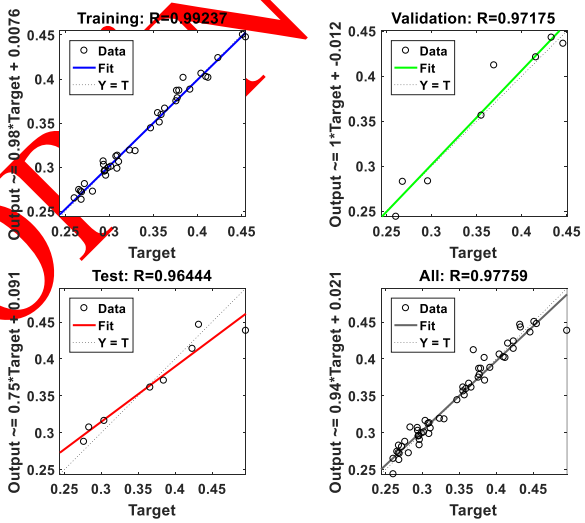

Figure 17. Regression Plot of COF

This high level of agreement suggests that the ANN model is highly accurate in predicting the outcomes under the given conditions and parameters.

Figure 17 showcases the regression graph of the ANN model for the COF across training, validation, test, and all data sets. The graph reveals that the coefficient of determination (R^2) for the training dataset is 0.99237, for validation is 0.9717, for testing is 0.96444, and the overall model coefficient is 0.9775. Similar to the mass loss regression graph, the COF regression graph also demonstrates that all coefficients of determination are very close to 1. This indicates a strong correlation between the experimental results and the predictions made by the ANN model, suggesting that the model is highly effective in predicting both COF and mass loss. These findings reinforce the capability of the developed ANN model in accurately predicting wear parameters. Sharma and colleagues have reported that optimum COF and wear rate values were achieved at the lowest load in filled GFRCs. They indicated that the most influential

parameters on wear rate, as determined by ANOVA analysis, were the filler material and the load.

Their ANN model, employing the Levenberg-Marquardt algorithm, closely matched the predicted COF values with experimental results, further validating the effectiveness of ANN models in such applications [10].

Table 7 displays the experimental and predicted mass loss and COF values for GFRC and CFRC under various wear conditions. When analyzing the results for COF and mass loss in relation to wear parameters, it is observed that the ANN predictions are closer to the experimental results compared to the Taguchi method. When Table 7 analyzed, it was determined that there were 11 prediction values for COF showing a deviation greater than 5% in the analysis conducted using the Taguchi method. However, in the analysis conducted with ANN, this number was reduced to 6. The experimental, Taguchi, and ANN COF values for glass fiber under a load of 5 N, a sliding distance of 250 m, and a sliding speed of 0.4 m/s are 0.2947 μ, 0.26 μ, and 0.30 μ, respectively. This comparison indicates that the ANN method is more successful than the Taguchi method in predicting the experimental outcomes for both mass loss and COF. Such findings highlight the effectiveness of ANN models in accurately predicting wear characteristics of composite materials. The ability of ANN to closely match the experimental data demonstrates its potential as a powerful tool in the analysis and design of materials, particularly in applications where understanding and optimizing wear properties are critical.

In Figure 18, a comparison is shown between the experimental results and the predicted values of COF and mass loss for CFRC under different loads, using both the Taguchi method and ANN. It is observed that the COF prediction curve from the ANN almost perfectly overlaps with the experimental result curve, indicating a high level of accuracy in the ANN predictions. On the other hand, the estimated values obtained from the Taguchi method show some deviation from the experimental values. This suggests that while the Taguchi method provides valuable insights, ANN predictions are more closely aligned with the actual experimental outcomes. Similarly, in the case of mass loss, the ANN predictions are again observed to be closer to the experimental results, mirroring the pattern seen in the COF graph. This consistency further validates the effectiveness of the ANN model in accurately predicting wear characteristics in composite materials, particularly in comparison to the Taguchi method. The ability of ANN to closely match experimental data underscores its utility as a reliable predictive tool in material science and engineering applications. When examining the experimental results in Table 7, it is observed that wear losses increase with increasing load in both glass fiber and carbon fiber reinforced composites. The increase in load leads to an increase in temperature due to the increased contact of the composite with the abrasive material, and as a result, the softening of the epoxy material makes it easier for the material to detach, thereby increasing the amount of wear [47]. Kim et al. emphasized that if the applied load exceeds a certain level, wear loss will increase logarithmically. They stated that the increase in stress on the contact area with the increase in load and the rise in temperature further increase material loss [48]. An increase in mass loss was also observed with an increase in sliding distance. In other similar studies, it has been emphasized that an increase in sliding distance leads to an increase in wear volume due to the increase in contact time with the abrasive material [49,50,51].

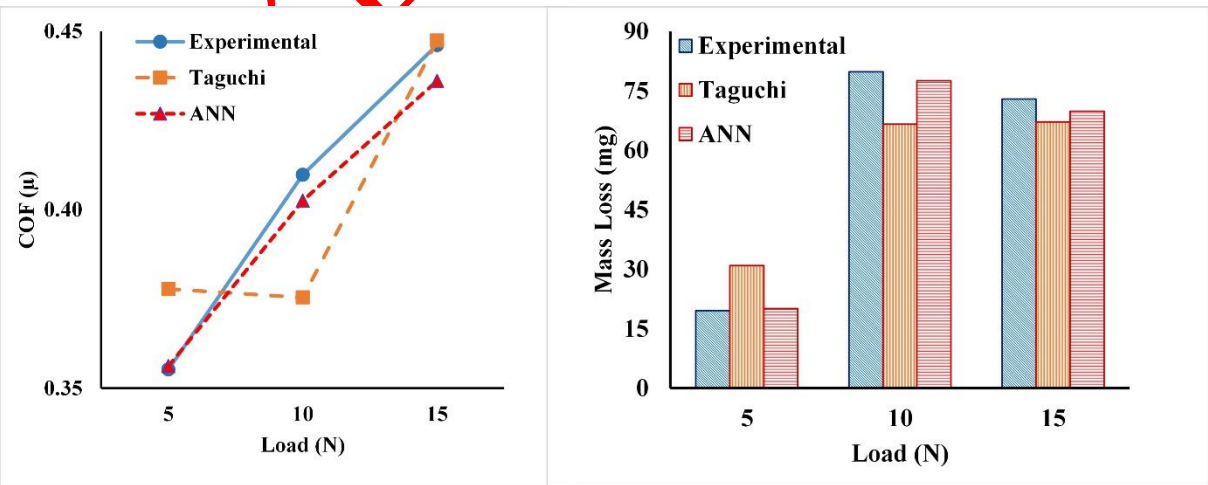

Figure 18. Comparison of experimental and predicted values of COF and mass loss

Table 7. Comparison of experimantal, Taguchi and ANN prediction results

CT	L	SD	Sd	COF (μ)	Predicted Taguchi COF	COF Error Taguchi (%)	Predicted ANN COF	COF Error ANN(%)	Mass Loss (mg)	Predicted Taguchi Mass Loss	Mass Loss Error Taguchi (%)	Predicted ANN Mass Loss	Mass Loss Error ANN(%)
GFRC	5	250	0.4	0.29	0.26	10.81	0.30	0.23	11.20	-8.59	176.68	11.24	0.33
GFRC	10	500	0.6	0.27	0.27	1.05	0.26	1.95	23.50	31.96	36.02	22.93	2.41
GFRC	15	750	0.8	0.32	0.34	4.18	0.32	1.31	51.70	59.12	14.36	51.32	0.73
GFRC	5	250	0.4	0.29	0.26	10.81	0.30	0.23	11.20	-8.59	176.68	11.24	0.33
GFRC	10	500	0.6	0.27	0.27	1.05	0.26	1.95	23.50	31.96	36.02	22.93	2.41
GFRC	15	750	0.8	0.32	0.34	4.18	0.32	1.31	51.70	59.12	14.36	51.32	0.73
GFRC	5	250	0.6	0.27	0.27	1.88	0.28	3.24	8.00	1.49	81.34	5.81	27.39
GFRC	10	500	0.8	0.28	0.29	1.80	0.31	8.38	33.70	42.01	24.67	32.37	3.96
GFRC	15	750	0.4	0.30	0.31	3.62	0.30	0.12	42.60	38.99	8.47	42.84	0.56
GFRC	5	250	0.8	0.30	0.29	2.09	0.29	1.92	14.10	11.54	18.14	14.02	0.56
GFRC	10	500	0.4	0.26	0.26	0.34	0.24	6.37	33.70	21.88	35.07	33.33	1.11
GFRC	15	750	0.6	0.29	0.31	6.98	0.31	4.54	40.60	49.08	20.88	29.11	28.31
GFRC	5	500	0.8	0.29	0.29	0.53	0.30	0.19	19.30	23.65	22.56	20.13	4.31
GFRC	10	750	0.4	0.30	0.26	13.17	0.26	11.38	42.60	29.11	31.66	38.53	9.56
GFRC	15	250	0.6	0.30	0.31	5.75	0.30	0.20	17.90	29.73	66.09	17.85	0.25
GFRC	5	500	0.8	0.29	0.29	0.53	0.30	0.19	19.30	23.65	22.56	20.13	4.31
GFRC	10	750	0.4	0.26	0.26	0.40	0.26	1.65	24.80	29.11	17.40	38.53	55.35
GFRC	15	250	0.6	0.30	0.31	5.75	0.30	0.20	17.90	29.73	66.09	17.85	0.25
CFRC	5	500	0.4	0.36	0.38	6.35	0.36	0.26	19.58	30.91	57.89	20.09	2.59
CFRC	10	750	0.6	0.41	0.38	8.39	0.40	1.78	79.80	66.59	16.56	77.56	2.80
CFRC	15	250	0.8	0.45	0.45	0.28	0.44	2.25	72.89	67.17	7.85	69.83	4.20
CFRC	5	500	0.6	0.36	0.38	7.56	0.36	1.80	37.80	41.00	8.45	37.71	0.23
CFRC	10	750	0.8	0.38	0.40	3.76	0.40	4.55	81.10	76.64	5.50	80.19	1.12
CFRC	15	250	0.4	0.43	0.42	2.79	0.45	3.30	41.60	47.04	13.08	37.61	9.59
CFRC	5	750	0.6	0.40	0.38	6.00	0.41	0.46	46.65	48.23	3.38	46.76	0.24
CFRC	10	250	0.8	0.37	0.40	7.55	0.41	11.57	55.40	57.29	3.41	55.52	0.21
CFRC	15	500	0.4	0.43	0.42	2.25	0.44	2.24	50.44	59.15	17.27	50.94	0.98
CFRC	5	750	0.6	0.40	0.38	6.00	0.41	0.46	46.65	48.23	3.38	46.76	0.24
CFRC	10	250	0.8	0.37	0.40	7.55	0.41	11.57	55.40	57.29	3.41	55.52	0.21
CFRC	15	500	0.4	0.43	0.42	2.25	0.44	2.24	50.44	59.15	17.27	50.94	0.98
CFRC	5	750	0.8	0.41	0.40	2.22	0.40	2.58	54.43	58.28	7.08	54.44	0.03
CFRC	10	250	0.4	0.36	0.37	3.03	0.36	0.07	27.39	37.16	35.67	27.24	0.56
CFRC	15	500	0.6	0.42	0.43	0.95	0.42	0.09	88.70	69.23	21.95	88.59	0.13
CFRC	5	750	0.4	0.35	0.38	8.29	0.34	0.83	33.61	38.15	13.51	33.34	0.79
CFRC	10	250	0.6	0.38	0.37	0.47	0.37	0.27	41.60	47.24	13.56	52.88	27.11
CFRC	15	500	0.8	0.50	0.45	9.13	0.44	11.59	92.37	79.28	14.17	92.31	0.06

CT: Composite type, L: Load, SD: Sliding distance, Sd: Sliding speed

4. CONCLUSION

The experimental results and analytical predictions from DOE and ANN regarding the wear behavior of GFRC and CFRC under varying parameters can be summarized as follows:

- It has been observed that increases in load, speed, and sliding distance have a negative effect on both the COF and mass loss. At a sliding speed of 0.6 m/s and a sliding distance of 250 m, the lowest COF value in GFRC at 5 N load was 0.27 μ, while the highest COF in CFRC at 15 N load was 0.45 μ. CFRC experienced more mass loss than GFRC.
- According to the S/N ratio, the most influential parameters on COF were, in order, fiber type, load, sliding speed, and sliding distance.
- The optimum mass loss values in the Taguchi experimental design were achieved at a load of 5 N, sliding distance of 250 m, and sliding speed of 0.4 m/s. The effect of sliding distance on COF was less significant compared to its impact on mass loss.
- For GFRC, the lowest COF of 0.260506 μ was obtained at 10 N load, 500 m sliding distance, and 0.4 m/s sliding speed. In tests conducted for CFRC according to Taguchi design, COF values ranged between 0.3552 and 0.4958, while mass losses varied from 19.58 mg to 92.37 mg.
- The ANN predicted values were found to be very close to the experimental results, indicating high accuracy. The R^2 regression coefficient for COF was 0.98939 and for mass loss was 0.98349, demonstrating the effectiveness of ANN in modeling these parameters.
- The predictions from the Taguchi method were not as precise as those from ANN, indicating

that ANN may be a more suitable tool for predicting these specific wear behaviors in composite materials.

DECLARATION OF ETHICAL STANDARDS

The author of this article declare that the materials and methods used in this study do not require ethical committee permission and/or legal-special permission

AUTHORS' CONTRIBUTIONS

Mehmet Emin DEMİR: Perofrmed the experiments and analyse the results. Wrote the manuscript.

CONFLICT OF INTEREST

There is no conflict of interest in this study.

REFERENCES

[1] Divya, G.S., and Suresha, B., "Role of Metallic Nanofillers on Mechanical and Tribological Behaviour of Carbon Fabric Reinforced Epoxy Composites", ***Materials Sciences and Applications***, 740–750 (2018).

[2] Lin, G. M., Xie, G. Y., Sui, G. X., and Yang, R., "Hybrid effect of nanoparticles with carbon fibers on the mechanical and wear properties of polymer composites", ***Composites Part B: Engineering,*** 43(1), 44-49, (2012).

[3] Yılmaz, H., Altın, Y., and Bedeloğlu, A., "Investigation of properties of graphene reinforced epoxy nanocomposites", ***Journal Of Polytechnic,*** 24(4), 1719-1727.(2021)

[4] Kaya, Z., Balcıoğlu, E., and Gün, H., "Fiber Takviyeli Kompozitlerin Farklı Deformasyon Hızındaki Mod I ve Mod I/II Kırılma Davranışların İncelenmesi. ***Journal Of Polytechnic***, 25(2), 843-853, (2022).

[5] Korku, M., Feyzullahoğlu, E., and Ilhan, R., "Investigation of the Effects of Environmental Conditions on Wear Behaviors in Glass Fiber Reinforced Polyester Composite Materials Containing Different Types of Polyester and Low Profile Additive", ***Journal Of Polytechnic,*** (2022).

[6] Sathishkumar, T. P., Satheeshkumar, S., and Naveen, J., "Glass fiber-reinforced polymer composites-A review", ***Journal of Reinforced Plastics and Composites***, 33(13): 1258–1275, (2014).

[7] Demir, M. E., Çelik, Y. H., and Kılıçkap, E., "Effect of fiber type, load, sliding speed and distance on abrasive wear of glass and carbon fiber reinforced composites", ***Journal Of Polytechnic***, *22*(4), 811-817, (2019).

[8] Suresha, B., Chandramohan G., Samapthkumaran, P., Seetharamu, S., and Vynatheya S., "Friction and wear characteristics of carbon-epoxy and glass-epoxy woven roving fiber composites", ***Journal of Reinforced Plastics and Composites,*** 25(7): 771–782, (2006).

[9] Srinath, G., and Gnanamoorthy, R., "Effect of short fibre reinforcement on the friction and wear behaviour of nylon 66", ***Applied Composite Materials,*** 12(6): 369–383, (2005).

[10] Sharma, N., Kumar, S., & Singh, K. K., "Taguchi's DOE and artificial neural network analysis for the prediction of tribological performance of graphene nano-platelets filled glass fiber reinforced epoxy composites under the dry sliding condition", ***Tribology International***, 172, 107580, (2022).

[11] Singh, K. K., Singh, N. K., and Jha, R., "Analysis of symmetric and asymmetric glass fiber reinforced plastic laminates subjected to low-velocity impact", ***Journal of composite materials,*** *50*(14), 1853-1863. (2016).

[12] Agrawal, S., Singh, K. K., and Sarkar, P. K., "A comparative study of wear and friction characteristics of glass fibre reinforced epoxy resin, sliding under dry, oil-lubricated and inert gas environments", ***Tribology International,*** 96, 217-224. (2016).

[13] Findik, F., Yilmaz, R., and Köksal, T., "Investigation of mechanical and physical properties of several industrial rubbers", ***Materials & design***, 25(4), 269-276. (2004).

[14] Çetkin, E., Demir, M. E., & Ergün, R. K., "The effect of different fillers, loads, and sliding distance on adhesive wear in woven e-glass fabric composites", ***Proceedings of the Institution of Mechanical Engineers, Part E: Journal of Process Mechanical Engineering,*** 237(2), 418-429, (2023).

[15] Kumar, S., & Ghosh, S. K., "Statistical and computational analysis of an environment-friendly MWCNT/NiSO4 composite materials", ***Journal of Manufacturing Processes,*** 66, 11-26, (2021).

[16] Gyurova, L. A., and Friedrich, K., "Artificial neural networks for predicting sliding friction and wear properties of polyphenylene sulfide composites", ***Tribology International,*** 44(5), 603-609, (2011).

[17] Jiang, Z., Zhang, Z., and Friedrich, K., "Prediction on wear properties of polymer composites with artificial neural networks", ***Composites Science and Technology,*** 67(2), 168-176, (2007).

[18] Ciurana, J., Quintana, G., and Garcia-Romeu, M. L., "Estimating the cost of vertical high-speed machining centres, a comparison between multiple regression analysis and the neural networks approach", ***International Journal of Production Economics***, 115(1), 171-178, (2008).

[19] Shtub, A., and Versano, R., "Estimating the cost of steel pipe bending, a comparison between neural networks and regression analysis", ***International Journal of Production Economics***, 62(3), 201-207, (1999).

[20] Padhi, P. K., Satapathy, A., and Nakka, A. M., "Processing, characterization, and wear analysis of short glass fiber-reinforced polypropylene composites filled with blast furnace slag", ***Journal of Thermoplastic Composite Materials***, 28(5), 656-671, (2015).

[21] Vaddar, L., Thatti, B., Reddy, B. R., Chittineni, S., Govind, N., Vijay, M, Saleel, C. A., "Glass Fiber-Epoxy Composites with Carbon Nanotube Fillers for Enhancing Properties in Structure Modeling and Analysis Using Artificial Intelligence Technique", ***ACS Omega***, (2023).

[22] Kumar, S., Sharma, N., and Singh, K. K., "Artificial Neural Network technique to assess tribological performance of GFRP composites incorporated with graphene nano-platelets", ***Tribology International,*** 179, 108194, (2023).

[23] Demir, M. E., Cetkin, E., Ergün, R. K., and Denizhan, O. "Tribological and mechanical properties of nanofilled glass fiber reinforced composites and analyzing the tribological behavior using artificial neural networks", ***Polymer Composites,*** (2024).

[24] Yadav, R., Lee, H. H., Meena, A., and Sharma, Y. K., "Effect of alumina particulate and E-glass fiber reinforced epoxy composite on erosion wear behavior using Taguchi orthogonal array", ***Tribology International***, 175, 107860, (2022)

[25] Kumar, M. S., Raju, N. M. S., Sampath, P. S., and Vivek, U., "Tribological analysis of nano clay/epoxy/glass fiber by using Taguchi's technique", ***Materials & Design***, 70, 1-9. (2015).

[26] Paturkar, A., Mache, A., Deshpande, A., and Kulkarni, A., "Experimental investigation of dry sliding wear behaviour of jute/epoxy and jute/glass/epoxy hybrids using Taguchi approach" ***Materials Today: Proceedings,*** 5(11), 23974-23983, (2018).

[27] Ravichandran, G., Rathnakar, G., Santhosh, N., and Suresh, R., "Wear characterization of HNT filled glass-epoxy composites using Taguchi's design of experiments and study of wear morphology", ***Composites Theory and Practice***, 20(2), 85-91, (2020).

[28] Bagci, M., Imrek, H., and Mashi Khalfan, O., "Optimization of test parameters that influence erosive wear behaviors of glass fiber-reinforced epoxy composites by using the Taguchi method", ***Journal of Tribology,*** 137(1), 011602, (2015).

[29] Thimmaiah, S. H., Narayanappa, K., Thyavihalli Girijappa, Y., Gulihonenahali Rajakumara, A., Hemath, M., Thiagamani, S. M. K., and Verma, A., "An artificial neural network and Taguchi prediction on wear characteristics of Kenaf–Kevlar fabric reinforced hybrid polyester composites", ***Polymer Composites,*** 44(1), 261-273, (2023).

[30] Demir, M. E., Çelik, Y. H., and Kilickap, E., "Effect of matrix material and orientation angle on tensile and tribological behavior of jute reinforced composites", ***Materials Testing,*** 61(8), 806-812, (2019).

[31] Unal, H., Mimaroglu, A., Kadıoglu, U., and Ekiz, H., "Sliding friction and wear behaviour of polytetrafluoroethylene and its composites under dry conditions", ***Materials & Design***, 25(3), 239-245, (2004).

[32] Sarkar, P., Modak, N., & Sahoo, P., "Effect of normal load and velocity on continuous sliding friction and wear behavior of woven glass fiber reinforced epoxy composite", ***Materials Today: Proceedings,*** 4(2), 3082-3092, (2017).

[33] Sumer, M., Unal, H., and Mimaroglu, A., "Evaluation of tribological behaviour of PEEK and glass fibre reinforced PEEK composite under dry sliding and water lubricated conditions", ***Wear,*** 265(7-8), 1061-1065, (2008).

[34] Ahmed, K. S., Khalid, S. S., Mallinatha, V., and Kumar, S. A., "Dry sliding wear behavior of SiC/Al2O3 filled jute/epoxy composites", ***Materials & Design***, 36, 306-315, (2012).

[35] Stuart, B. H., "Surface plasticisation of poly (ether ether ketone) by chloroform", ***Polymer testing,*** 16(1), 49-57, (1997).

[36] Davim, J. P., and Cardoso, R. "Effect of the reinforcement (carbon or glass fibres) on friction and wear behaviour of the PEEK against steel surface at long dry sliding", ***Wear***, 266(7-8), 795-799, (2009).

[37] Yousif, B.F., and Yap, T.C., "Tribological studies of polyester reinforced with CSM 450-R-glass fiber sliding against smooth stainless steel counterface",***Wear,*** 261 443–452 (2006).

[38] Suresha, B., "Friction and dry slide wear of short glass fiber reinforced thermoplastic polyurethane composites", ***Journal of reinforced plastics and composites***, 29(7), 1055-1061, (2010).

[39] Suresha, B., Chandramohan, G., Samapthkumaran, P., & Seetharamu, S., "Three-body abrasive wear behaviour of carbon and glass fiber reinforced epoxy composites", ***Materials Science and Engineering: A,*** 443(1-2), 285-291, (2007).

[40] Chen, B., Wang, J., & Yan, F., "Comparative investigation on the tribological behaviors of CF/PEEK composites under sea water lubrication", ***Tribology International,*** 52, 170-177, (2012).

[41] Lin, G., Xie, G., Sui, G., and Yang, R., "Hybrid effect of nanoparticles with carbon fibers on the mechanical and wear properties of polymer composites", ***Composites Part B***, 43 (1), 44–49 (2012).

[42] Agarwal, G., Patnaik, A., and Sharma, R. K., "Comparative investigations on three-body abrasive wear behavior of long and short glass fiber-reinforced epoxy composites", ***Advanced Composite Materials,*** 23(4), 293-317, (2014).

[43] Davim, J.P. and Cardoso, R., "Effect of the reinforcement (carbon or glass fibres) on friction and wear behaviour of the PEEK against steel surface at long dry sliding", ***Wear***, 266 (7–8), 795–799, (2009).

[44] Srinivasan, V., Karthikeyan, R., Ganesan, G., and Asaithambi, B. "Comparative Study on the Wear Behavior of Long and Short Glass Fiber Reinforced Plastics", ***Metals and Materials International***, 16 (2), 205–212, (2010).

[45] Baday, Ş., Ersöz, O., "Comparative investigations of cryo-treated and untreated inserts on machinability of AISI 1050 by using response surface methodology, ANOVA and Taguchi design", ***Proceedings of the Institution of Mechanical Engineers, Part C: Journal of Mechanical Engineering Science,*** 236(3), 1751-1765, (2022).

[46] Denizhan, O., "Comparison of different supervised learning algorithms for position analysis of the slider-crank mechanism", ***Alexandria Engineering Journal,*** 92, 39-49, (2024).

[47] Arun, A., and Kalyan K. S., "Friction and wear behaviour of glass fibre reinforced polymer composite (GFRP) under dry and oil lubricated environmental conditions", ***Materials Today: Proceedings***, 4(8) 7285-7292, (2017).

[48] Kim, S. S., Shin, M. W., and Jang, H., "Tribological properties of short glass fiber reinforced polyamide 12 sliding on medium carbon steel", ***Wear,*** 274, 34-42, (2012).

[49] Sharma, V., Meena, M. L., Kumar, M., & Patnaik, "A., Waste fly ash powder filled glass fiber reinforced epoxy composite: physical, mechancial, thermo-mechanical, and three-body abrasive wear analysis", ***Fibers and Polymers***, 22(4), 1120-1136, (2021).

[50] Suresha, B., & Kumar, K. N. S., "Investigations on mechanical and two-body abrasive wear behaviour of glass/carbon fabric reinforced vinyl ester composites", ***Materials & Design,*** 30(6), 2056-2060, (2009).

[51] Şahin, Y., and Patrick, D. B., "Effects of nano-Al2O3 and PTFE fillers on tribological property of basalt fabric-reinforced epoxy composites", ***Tribology-Materials, Surfaces & Interfaces,*** 15(4), 258-277, (2021).

[52] Wen, Q., Liu, M., Zhang, Z., & Sun, Y., "Experimental investigation into the friction coefficient of ball-on-disc in dry sliding contact considering the effects of surface roughness, low rotation speed, and light normal load", **Lubricants**, 10(10), 256, (2022).

[53] Singh, M., Dodla, S., Gautam, R. K., & Srivastava, V. K., "Effect of load, sliding frequency, and temperature on tribological properties of graphene nanoplatelets coated carbon fiber reinforced polymer composites", **Journal of Composite Materials**, 57(1), 121-132, (2023).

[54] Yelmen, B., Çakır, M. T., Şahin, H. H., Kurt, C., "Yapay Sinir Ağı (YSA) Kullanarak Sera Sistemlerinde Enerji Verimliliğinin Modellenmesi", **Journal Of Polytechnic**, 24(1), 151-160, (2021).

[55] Toktaş İ., "Eliptik delikli ince cidarlı küresel bir elemanın basınç altında gerilme yığılma faktörünün sonlu elemanlar analizi ve yapay sinir ağları ile modellenmesi", **Journal Of Polytechnic**, 27(2): 819-827, (2024).

[56] Gürbüz G., Gönülaçar Y. E., "Farklı kesme parametreleri ve MQL debilerinde elde edilen deneysel değerlerin S/N oranları ve YSA ile analizi", Politeknik Dergisi, 24(3): 1093-1107, (2021).

[57] Erdoğan, M., ve Yıldız O., "Evrişimli sinir ağı kullanarak dengesiz doppler radar verisinde hedef tespiti", **Journal of Polytechnic,** (2023).